Characterising Desktop Colour Printers Without Full Control Over All Colorants

Ján Morovic and M. Ronnier Luo
Design Research Centre, University of Derby, United Kingdom

Abstract

This paper describes the results of work carried out on characterising desktop colour printers which do not enable the control of device colorant amounts independently and individually. As this particular limitation is shared by the majority of colour printers available to date, their characterisation is important especially in light of the development of gamut mapping algorithms. Four characterisation models have been implemented and tested for this purpose: a third order masking model, a model using separate masking equations for different parts of the colour space, a fourth order masking model and a model using distance weighted interpolation. The results of the experiments described in this paper suggest that the fourth order masking model is most suitable for the reproduction of complex images.

Introduction

In the last decade, substantial progress has been made in the development of device characterisation models, colour appearance models and gamut mapping algorithms—the components of a colour reproduction system based on colour science.[1] For such a system to be successful, the assumptions made at each stage need to be fulfilled by the environment in which it is implemented. In particular, the assumption made by the characterisation models developed to date is that it is possible to control a device's colorants individually and independently. This, however, is not the case for the majority of desktop printing devices available at the moment and as these devices could be used in most colour reproduction systems, this paper looks at their characterisation. A description of the chosen characterisation models can be found in the following sections alongside the details and results of experiments carried out to establish their performance.

Characterisation Models

As the four colorants used by most colour printers cannot be controlled individually and black generation is carried out by the printer automatically and unalterably, the characterisation can be regarded as being a transformation between the cyan, magenta and yellow (CMY) values sent to the printer and the tristimulus values of the resulting printed colour. Even though the 'virtual' CMY values considered here are not those directly output by the printer, they still are the most practical correlates available for them.

The characterisation of colour printers described here forces their treatment as "black boxes," therefore it is paramount to adjust their settings carefully, as certain settings on some desktop printers make their colorimetric characterisation virtually impossible.

Third Order Masking Model

This characterisation model is a well established one and dates back to Clapper's work in 1961.[2] Its aim is to describe the relationship between tristimulus values and colorant amounts using a set of three third order equations. The first of the three equations is as follows:

$$\begin{aligned} C = {} & \alpha_{11}D_r + \alpha_{12}D_g + \alpha_{13}D_b + \alpha_{14}D_r^2 + \alpha_{15}D_g^2 + \\ & \alpha_{16}D_b^2 + \alpha_{17}D_rD_g + \alpha_{18}D_rD_b + \alpha_{19}D_gD_b + \\ & \alpha_{110}D_r^3 + \alpha_{111}D_g^3 + \alpha_{112}D_b^3 + \alpha_{113}D_r^2D_g + \\ & \alpha_{114}D_r^2D_b + \alpha_{115}D_g^2D_r + \alpha_{116}D_g^2D_b + \\ & \alpha_{117}D_b^2D_r + \alpha_{118}D_b^2D_g \end{aligned} \tag{1}$$

Here C is the 'virtual' amount of cyan and D_r, D_g and D_b are the colorimetric densities which are obtained from measured tristimulus values using the formulæ $D_r = \log(X_0/X)$, $D_g = \log(Y_0/Y)$ and $D_b = \log(Z_0/Z)$. Analogous equations apply for the two other virtual colorants.

The 3×18 coefficients in these equations are calculated using the least–squares method, whereby the error is minimised for colours from a colour cube of arbitrary size (see Figure 1).

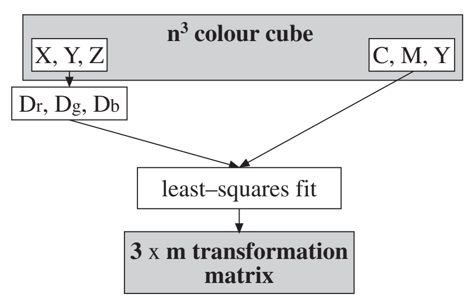

*Figure 1. Deriving the transformation matrix for the masking model (*n *is the size of the colour cube and* m *depends on the order of the equations and the number of terms used).*

As for all characterisation models, the matrices can be computed for both directions of transformation—XYZ to CMY and CMY to XYZ—however only the former transformations are discussed here.

Four Sector Model

This model is an extension of the previous one, whereby it tries to resemble the actual workings of the printer more closely. As desktop printers typically use black generation similar to 100% GCR, only three different colorant combinations are possible: CMK, CYK and MYK. This model therefore consists of three separate transformation matrices for each of these three sectors.

At the stage of calculating the transformation matrices from the colour cube data, the smallest of the CMY colorant amounts determines into which sector a particular colour belongs. When the actual XYZ to CMY transformation is carried out, the CIE LAB hue angle calculated from the XYZ tristimulus values determines which sector's transformation matrix to use. Even though the boundary is defined using a piece–wise linear function (see Figure 2), there are some problems as the boundaries between the sectors are not uniform for all lightness levels.

So far only three sectors have been described, however an additional sector is used for neutral colours as these would have a colour cast if reproduced using a three sector model. Those colours which have CIE LAB chroma smaller than 3.0 are thus transformed separately.

Even though this model resembles the printer more closely, its potential problem is that it could have inaccuracies in the border regions between the individual sectors and colours from one sector could be transformed using a different sector's matrix.

Fourth Order Masking Equations

This model is closely related to the third order masking model and all its implementation–related features (except for the masking equations themselves) are the same. Nine additional fourth order terms are added to the masking equations whereby we get new equations of the following kind:

$$\begin{aligned} C = {} & \alpha_{11}D_r + \alpha_{12}Dg + \alpha_{13}D_b + \alpha_{14}D_r^2 + \alpha_{15}D_g^2 + \\ & \alpha_{16}D_b^2 + \alpha_{17}D_rD_g + \alpha_{18}D_rD_b + \alpha_{19}D_gD_b + \\ & \alpha_{110}D_r^3 + \alpha_{111}D_g^3 + \alpha_{112}D_b^3 + \alpha_{113}D_r^2D_g + \\ & \alpha_{114}D_r^2D_b + \alpha_{115}D_g^2D_r + \alpha_{116}D_g^2D_b + \\ & \alpha_{117}D_b^2D_r + \alpha_{118}D_b^2Dg + \alpha_{119}D_r^2Dg^2 + \\ & \alpha_{120}D_r^2D_b^2 + \alpha_{121}D_g^2D_b^2 + \alpha_{122}D_r^3D_g + \\ & \alpha_{123}D_r^3D_b + \alpha_{124}D_g^3D_r + \alpha_{125}D_g^3D_b + \\ & \alpha_{126}D_b^3D_r + \alpha_{127}D_b^3D_r \end{aligned} \tag{2}$$

Again, the same notation applies as for the third order masking equations.

Distance Weighted Interpolation Model

The last model described here uses distance weighted interpolation as described originally by Shepard.[3] Even though this method is potentially less accurate than other interpolation methods used previously for characterisation purposes (e.g. tetrahedral interpolation), its advantage is that it works well even with non–monotonic data, which is often the case with desktop printers. To obtain the 'virtual' CMY values for a given set of CIE LAB coordinates, the following procedure is used:

1. A colour cube of arbitrary size is loaded.
2. Eight colours forming a sub–cube around the target LAB co–ordinates are found (for boundary colours only a smaller number can be located).
3. The distances between these eight colours and the target colour are used to compute weights using the following equation:

$$w_i = \frac{\sigma_i}{\sum_{j=1}^{8} \sigma_i}, \; where \; \sigma_i = \frac{1}{d_i^{\mu}} \tag{3}$$

here d_i is the distance of the ith colour from the target and the exponent μ determines the smoothness of the interpolation, whereby if $\mu > 1$ the first derivative is continuous. In this case μ has been set to 1.5, so as to achieve a smooth interpolation, however an optimisation of this exponent could give even better results.

4. To obtain the colorant amounts of the given LAB colour, the virtual colorant amounts of the eight colours are combined as follows:

$$C = \sum_{i=1}^{8} w_i C_i, M = \sum_{i=1}^{8} w_i M_i, Y = \sum_{i=1}^{8} w_i Y_i. \tag{4}$$

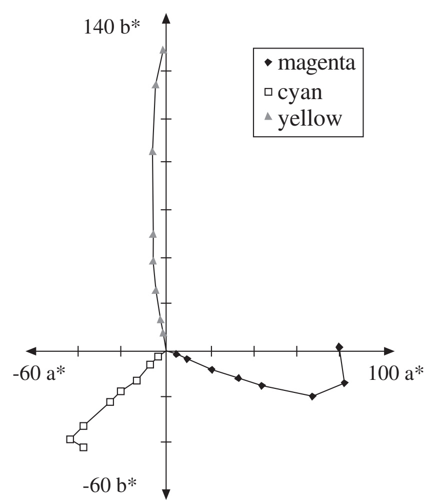

Figure 2. Boundaries of the three chromatic sectors.

Experimental Setup

To test the characterisation models described above, an office and home inkjet printer using coated paper has been characterised using each one of them. In addition to testing the models, the effect of the number of colours used for the modelling has also been examined. Four colour cubes have been used with three, four, five and nine levels per virtual colorant. The steps in these colour cubes have been chosen so as to be visually equal rather than to have the same difference in colorant value, as this had been found to give better results in an earlier study.[4,5] The following table shows the steps in colorant amount used for the four colour cubes:

Table 1. Colorant Levels Used in Colour cubes

Size	*Steps (%)*
$3\times3\times3$	0, 40 and 100
$4\times4\times4$	0, 20, 60 and 100
$5\times5\times5$	0, 10, 30, 60 and 100
$9\times9\times9$	0, 5, 10, 20, 30, 40, 60, 80 and 100

All the measurements in this experiment were carried out using an XRite 938 spectrophotometer, which has a determined repeatability of 0.3 ΔE and all colour differences are calculated using the CMC(1:1) formula.[6]

An additional $5\times5\times5$ colour cube has been generated and measured for testing purposes. The colorant steps in this cube were of equal colorant value difference (i.e. 0%, 25%, 50%, 75% and 100%), therefore only the eight primary colours were common to both the training and the testing sets.

To test the XYZ to CMY transformation, the 125 testing colours were transformed using the four models and the resulting CMY values were printed and measured. The colour differences shown in the results and appendix represent the difference between the original XYZ coordinates and the XYZ measurements of the calculated CMY values. This, however, means that they include not only the model errors but also the errors inherent in the printer itself, which in our case had an average of 1.5 ΔE with 1.4 ΔE being the standard deviation and 7.5 ΔE the maximum. These values represent the best possible precision achievable with any characterisation model.

Results

The assumption is often made that the errors of characterisation models have a normal distribution which means that the mean can be used as a measure of central tendency and the standard deviation as a measure of dispersion. However, if the error distribution is different in nature, as is the case with the results of this experiment (see Figure 3), then other descriptive statistics need to be applied.

To describe the above distribution more accurately, the median will be used as a measure of central tendency and the 95th percentile to describe the dispersion (this would correspond to the mean plus 1.64 units of standard deviation in a normal distribution).

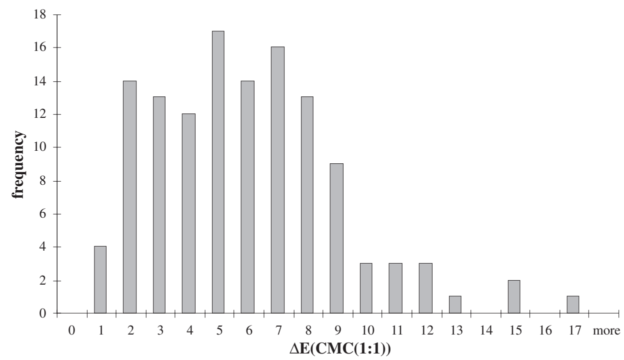

Figure 3. Histogram of errors from 4th order masking equations using 9×9×9 training cube

The results of the XYZ to CMY transformation are shown in figure 4 in terms of median, 95th percentile and maximum error. To provide a possibility for comparison with other experiments the mean and standard deviation are also shown in the appendix.

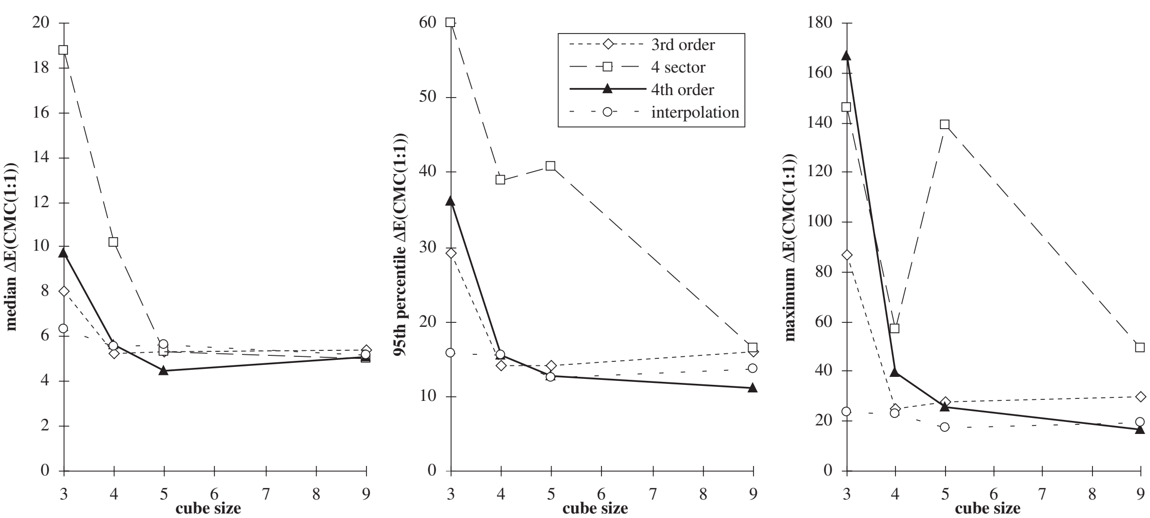

Figure 4. Descriptive statistics of characterisation model errors

From the above results it can be seen that the four sector model is clearly inferior to the other three. This is most probably due to the inadequate definition of the sector boundaries as well as due to the insufficient number of colours available to the least squares method for setting up four sets of third order equations.

Comparing the third and fourth order masking equation models derived from the $9 \times 9 \times 9$ cube, there is only a 0.3 ΔE improvement in terms of median, however the 95th percentile is reduced by 4 and the maximum error by 5 ΔE units when the higher order equations are used. Considering the size of the training colour cube, it is sufficient to use four steps per colorant if these steps are chosen appropriately. As can be seen from Figure 4, the increase in colour cube size mainly influences the dispersion of the colour differences while the mean is not affected significantly.

Finally, the distance–weighted interpolation gave the second best overall results and was least affected by the training cube size. Nonetheless, this method is not particularly suited to reproducing complex images as gradual transitions in input data are not reproduced monotonically. This is caused by the distance-weighting method shifting colours towards the centre of the sub-cube within which it interpolates. However, if only a small number of colours are available for setting up the characterisation model, this method gives the best results.

Conclusions

From the experiments described in this paper, the fourth order masking equations seem to be the most suitable model for characterising printers, where full control over the device's colorants is not possible. Even though the best median colour difference achievable with this model on the printer used is 5.08 ΔE, this is still adequate for the reproduction of complex images as a study by Stokes et al[7] suggests that colour differences on a pixel–by–pixel basis of up to 6 ΔE(LAB) are acceptable and colour differences of less than 3 ΔE(LAB) are not perceptible. Considering that the colour differences obtained by the models evaluated here are of the same order of magnitude and the small cost involved in acquiring and running printers of this kind, the results are encouraging.

Acknowledgements

We would like to thank Mr. Tony Johnson and Dr. Peter Rhodes for their helpful advice and suggestions.

Appendix – Detailed Results

Table 2. Summary of Characterisation Models' Tests (XYZ to CMY)

Average error				
model\cube size	*3*	*4*	*5*	*9*
3rd order	11.45	6.68	6.46	6.68
4 sector	22.42	13.67	10.84	6.32
4th order	14.55	6.71	6.03	5.47
interpolation	7.39	6.58	6.09	5.79
Standard deviation				
model\cube size	*3*	*4*	*5*	*9*
3rd order	12.02	4.46	4.37	5.03
4 sector	21.44	11.83	18.67	6.09
4th order	20.10	5.53	4.63	3.13
interpolation	4.54	4.41	3.35	3.86
Median				
model\cube size	*3*	*4*	*5*	*9*
3rd order	8.06	5.25	5.35	5.41
4 sector	18.75	10.20	5.36	5.04
4th order	9.73	5.62	4.51	5.08
interpolation	6.30	5.59	5.62	5.14
95th percentile				
model\cube size	*3*	*4*	*5*	*9*
3rd order	29.11	14.20	14.04	16.09
4 sector	59.91	38.90	40.71	16.48
4th order	36.11	15.41	12.67	11.06
interpolation	15.77	15.63	12.59	13.63
Maximum				
model\cube size	*3*	*4*	*5*	*9*
3rd order	87.15	24.89	27.62	29.65
4 sector	146.20	56.96	139.09	49.20
4th order	166.85	39.43	25.88	16.47
interpolation	23.80	22.65	17.12	19.66

References

1. M. R. Luo and J. Morovic, Two Unsolved Issues in Colour Management–Colour Appearance and Gamut Mapping, *Proceedings of 5th International Conference on High Technology: Imaging Science and Technology – Evolution & Promise*, 1996, Chiba, Japan.
2. F. R. Clapper, An Empirical Determination of Half–tone Colour Reproduction Requirements, *TAGA Proceedings*, pp. 31–41 (1961).
3. D. Shepard, A Two–Dimensional Interpolation Function for Irregularly Spaced Data, *Proc. 23rd National Conference of the ACM*, ACM Press, pp. 517–524 (1968).
4. A. Johnson, M. R. Luo, M. Lo, J. H. Xin and P. A. Rhodes, Aspects of Colour Management. Part I–Characterisation of Three–Colour Imaging Devices in Color Research and Application, *Colour Research and Application*, vol. **22**, pp. 000–000, (1997).
5. A. Johnson, M. R. Luo, M. Lo, J. H. Xin and P. A. Rhodes, Aspects of Colour Management, Part II Characterisation of Four–Colour Imaging Devices and Colour Gamut Compression, *Colour Research and Application*, vol. **22**, pp. 000–000, (1997).
6. F. J. J. Clarke, R. MacDonald and B. Rigg, Modification of the JPC79 Colour–Difference Formula, *J. Soc. Dyers Col.* **100**, pp. 117, (1984)
7. M. Stokes, M. D. Fairchild and R. S. Berns, Colorimetrically Quantified Visual Tolerances for Pictorial Images, *TAGA/ISCC Proc.* Vol. **2**, pp. 757–777 (1992